

# Transcainide Causes Two Modes of Open-Channel Block with Different Voltage Sensitivities in Batrachotoxin-Activated Sodium Channels

Gerald W. Zamponi and Robert J. French

Department of Medical Physiology and the Neuroscience Research Group, University of Calgary, Calgary, Alberta T2N 4N1, Canada

**ABSTRACT** Transcainide, a complex derivative of lidocaine, blocks the open state of BTX-activated sodium channels from bovine heart and rat skeletal muscle in two distinct ways. When applied to either side of the membrane, transcainide caused discrete blocking events a few hundred milliseconds in duration (slow block), and a concomitant reduction in apparent single-channel amplitude, presumably because of rapid block beyond the temporal resolution of our recordings (fast block). We quantitatively analyzed block from the cytoplasmic side. Both modes of block occurred via binding of the drug to the open channel, approximately followed 1:1 stoichiometry, and were similar for both channel subtypes. For slow block, the blocking rate increased, and the unblocking rate decreased with depolarization, yielding an overall enhancement of block at positive potentials, and suggesting a blocking site at an apparent electrical distance about 45% of the way from the cytoplasmic end of the channel ( $z\delta \approx 0.45$ ). In contrast, the fast blocking mode was only slightly enhanced by depolarization ( $z\delta \approx 0.15$ ). Phenomenologically, the bulky and complex transcainide molecule combines the almost voltage-insensitive blocking action of phenylhydrazine (Zamponi and French, 1994a (companion paper)) with a slow open-channel blocking action that shows a voltage dependence typical of simpler amines. Only the slower blocking mode was sensitive to the removal of external sodium ions, suggesting that the two types of block occur at distinct sites. Dose-response relations were also consistent with independent binding of transcainide to two separate sites on the channel.

## INTRODUCTION

Transcainide is a relatively new class I antiarrhythmic agent (Stroobandt et al., 1987). Although structurally related to lidocaine, the molecule is much bulkier than the lidocaine molecule, and its blocking kinetics, measured in ventricular myocytes, are much slower than those of lidocaine (Bennett et al., 1987) and more like those seen with flecainide and encainide (Carmeliet, 1988). After flecainide and encainide had been associated with an increased mortality rate of patients (CAST Investigators, 1989), the production of transcainide was discontinued (R. S. Sheldon, personal communication). However, the action of this compound is striking and unusual and, thus, has special biophysical interest.

In the preceding paper (Zamponi and French, 1994a), we have described the blocking actions of a variety of structurally related amines, including the two very similar molecules phenylmethanamine and phenylhydrazine, on BTX-activated cardiac sodium channels. Although both compounds caused rapid open-channel block, which appeared as a decrease in single-channel amplitude, block by phenylmethanamine was voltage-dependent ( $z\delta \approx 0.5$ ), whereas phenylhydrazine block showed little or no voltage dependence ( $z\delta \approx 0.1$ ). We proposed a mechanism in which binding of the aromatic ring to a putative hydrophobic site located in the vicinity of the narrow region of the pore prevents the charged amino ter-

minal of rigid, planar phenylhydrazine, but not that of the relatively flexible phenylmethanamine, from significant entry into the transmembrane voltage. Here, we show that transcainide is capable of two distinct modes of open-channel block, one slow and voltage-dependent, the other rapid and almost voltage-independent. We propose that, during fast block, transcainide binding to the putative aromatic site prevents significant entry of the charged portion of the blocker into the transmembrane electric field. During slow block, we envision that the molecule binds to an ionic site located more deeply inside the channel. A kinetic analysis indicates that slow block can occur while the channel is fast-blocked, suggesting a hydrophobic access to the slow block receptor.

## MATERIALS AND METHODS

Bilayer experiments were performed using symmetric 200 mM NaCl/20 mM MOPS at pH 7.0, as outlined in the preceding paper (Zamponi and French, 1994a). Membrane vesicle suspensions (2–3.5 mg/ml protein) from rat skeletal muscle and bovine cardiac tissue were prepared according to the protocols outlined by Guo et al. (1986). The vesicles were incubated with BTX as described previously (Zamponi et al., 1993a).

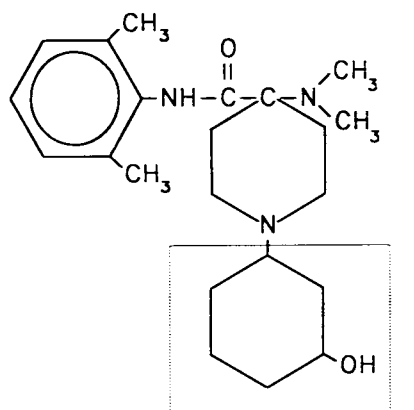
Transcainide was a gift from Drs. R. S. Sheldon and H. J. Duff, Department of Medicine, University of Calgary. The chemical structure of transcainide is displayed in Fig. 1. Note that the drug contains two tertiary amines, one at the terminal ( $pK_a = 8.9$ ) and a second amine that forms part of a saturated ring ( $pK_a = 3.7$ ) (Bennett et al., 1987). Under our experimental conditions (pH 7.0), only the terminal amine is charged. Transcainide was prepared as a stock solution of 50 mM transcainide/200 mM MOPS at pH 7.0 and simply added to either side of the channel to give final concentrations between 0.3 and 9 mM transcainide. Because transcainide is a highly hydrophobic molecule, we were unable, at a pH of 7.0, to make a drug stock solution with a concentration larger than 50 mM or add 200 mM NaCl to the transcainide stock. The relatively low stock concentration required the addition of relatively large stock volumes, resulting in a slight dilution of the recording solution (15% at the largest drug concentration used) and, hence, a small shift of the reversal potential. This complication could po-

Received for publication 14 March 1994 and in final form 26 May 1994.

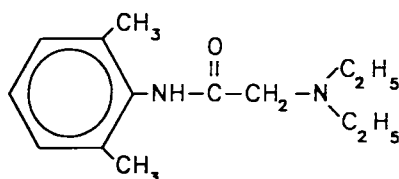
Address reprint requests to Dr. Robert J. French, Department of Medical Physiology, University of Calgary, 3330 Hospital Drive N.W., Calgary, Alberta T2N 4N1 Canada. Fax: 403-283-8731.

© 1994 by the Biophysical Society

0006-3495/94/09/1028/12 \$2.00



Transcainide



Lidocaine

FIGURE 1 Chemical structure of transcainide in comparison with the structure of lidocaine. Like lidocaine, transcainide carries an aromatic ring with two methyl groups, an aryl-amine link, and a terminal amino group ( $pK_a = 8.9$ ) that carries two alkyl chains. The major difference between the two molecules occurs in the aryl-amine link, where transcainide carries two bulky rings, one of which contains a second tertiary amino group ( $pK_a = 3.7$ ). The structure in the dashed box is shared with the batrachotoxin molecule.

tentially be avoided by generating drug stock solutions at the various final concentrations and simply perfusing the bilayer chamber. However, we were not able to obtain a transcainide sample large enough to make the required amounts of solution.

It has been previously reported that the internal sodium concentration has little effect on degree of block of BTX-activated sodium channels by a related compound, cocaine (Wang, 1988). In our analysis, fast block was evaluated from the reduction in normalized single-channel conductance,  $g/g(\text{drug free})$ , where  $g = i/(V_c - E_{rev})$ ,  $g$  is the single-channel conductance,  $i$  is the apparent single-channel amplitude,  $V_c$  is the command potential, and  $E_{rev}$  is the reversal potential. The estimated shifts in  $E_{rev}$ , calculated from the Nernst equation, at the various final transcainide concentrations were as follows: 1 mM, 0.49 mV; 3 mM, 1.47 mV; 6 mM, 2.85 mV; 9 mM, 4.24 mV. Given that these shifts are small, and that the  $i$  vs.  $V_c$  relations are nearly linear, use of single-channel conductance to evaluate fast block represents only a minor correction from the estimate that would be obtained directly from normalized single-channel current amplitudes.

Records (with  $300 \pm 180$  slow blocked events/experimental condition, mean  $\pm$  SD) were acquired in sweeps from 2 to 5 min under each condition. The data were filtered at 250 Hz and sampled at 500 Hz during transcription into a personal computer (Compaq 386). The mean durations of the gating and blocked events and the associated open probabilities were determined from events lists generated at a bandwidth of 50 Hz using pClamp software (Axon Instruments, Foster City, CA). No events were ignored during the creation of events lists; however, filtering at 50 Hz results in the loss of events shorter than 3.6 ms (McManus et al., 1987). We did not correct for missed events. To determine the degree of fast open-channel block, the apparent single-channel amplitude was measured by cursor and the single-

channel conductance calculated as described above. Least-squares fits to data, and preparation of figures, were carried out using Sigmaplot v. 5.0 (Jandel Scientific, Corte Madera, CA).

## RESULTS

### Transcainide causes two modes of block

Fig. 2 shows typical records obtained from one BTX-activated bovine cardiac and one rat skeletal muscle sodium channel in the absence and presence of 3 mM internal transcainide at a membrane potential of +40 mV. At this potential, both channel types showed an apparent single-channel amplitude of about 0.8 pA and were open most of the time in absence of the drug, but did show some spontaneous gating closures. Application of 3 mM internal transcainide resulted in the appearance of discrete blocking events with mean durations of about 0.5 s. Moreover, the apparent single-channel amplitude decreased to about 70% of the control value without a noticeable increase in open-channel noise, consistent with a very rapid, open-channel block beyond the temporal resolution of the recording. Both channel subtypes were similarly affected. We observed a qualitatively similar blocking behavior for application to the extracellular side of each of the channel subtypes (3 experiments on each channel type, data not shown); however, given the limited amount of drug available, we restricted our quantitative analysis to internal application of the drug.

For the purpose of this paper, we term the two blocking modes "slow" and "fast" block. Because the fast blocking mode was not resolved as discrete steps, the observed open state in the presence of transcainide shows a reduced single-channel amplitude as well as a slow block-induced reduction in life time. Hence, what we refer to as "open probability" is really the probability of not being in one of the closed or slow blocked states, and "mean open times" are strictly the durations between the adjacent closed and/or slow blocked events.

Both types of block were concentration-dependent. Fig. 3 A shows dose-response curves for slow block for one bovine cardiac and one rat skeletal muscle channel. The open probabilities of both channel subtypes decreased similarly with transcainide concentration. When the data were approximated with simple hyperbolas, the least-squares fits indicated apparent values for the equilibrium dissociation constants,  $K_d(\text{slow})$ , of 4.1 and 3.4 for the cardiac and the skeletal muscle subtypes, respectively. Fig. 3 B depicts dose-response curves for fast block from three experiments for each channel subtype. The data were fitted with simple hyperbolas, suggesting a 1:1 interaction between the channel and the transcainide molecule. The values for the equilibrium dissociation constants,  $K_d(\text{fast})$ , were 6.0 and 7.6 mM for the cardiac and the skeletal muscle channels, respectively, indicating a somewhat lower affinity than the slow blocking mode. Note that both channel subtypes were similarly affected by each blocking mode, similar to the lack of tissue specificity observed for open-channel block by lidocaine, QX-314 or procainamide (Zamponi et al., 1993a, b).

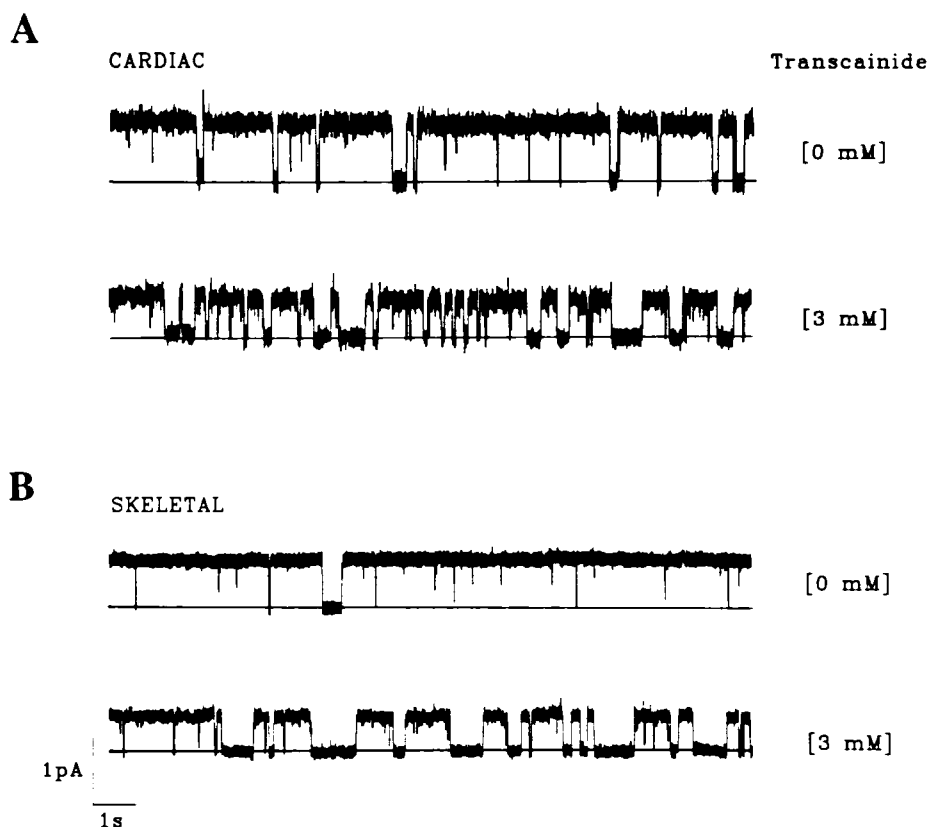


FIGURE 2 Single-channel records from BTX-activated cardiac (A) and skeletal muscle (B) sodium channels at a membrane potential of  $-40$  mV. The records were filtered at 50 Hz; solid lines indicate the closed level. In absence of blockers, the two channels were open most of the time. Application of 3 mM transcaïnide resulted in two distinct modes of open-channel block: discrete blocking events, and a concomitant reduction in apparent single-channel amplitude, without an apparent increase in noise. The effect of the drug was similar for both channel types.

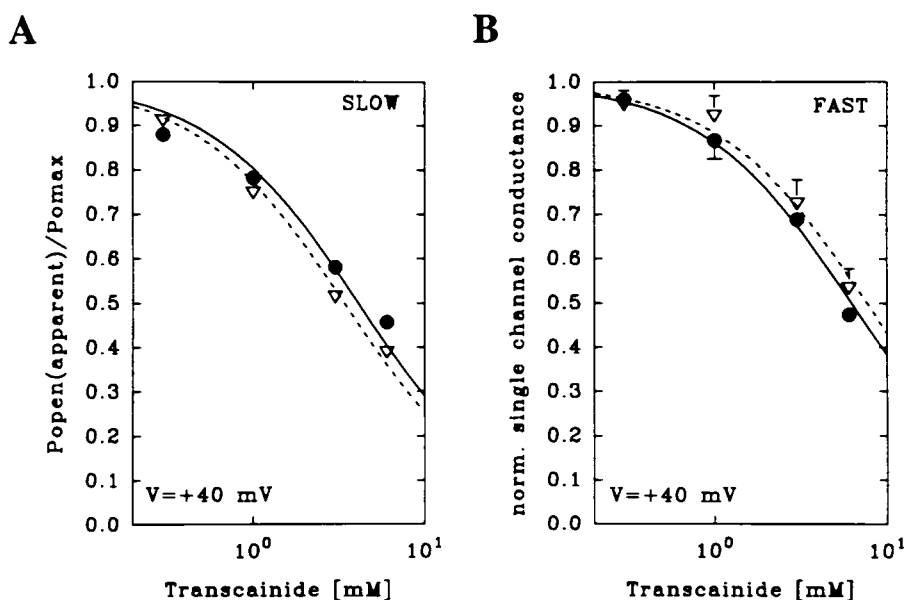
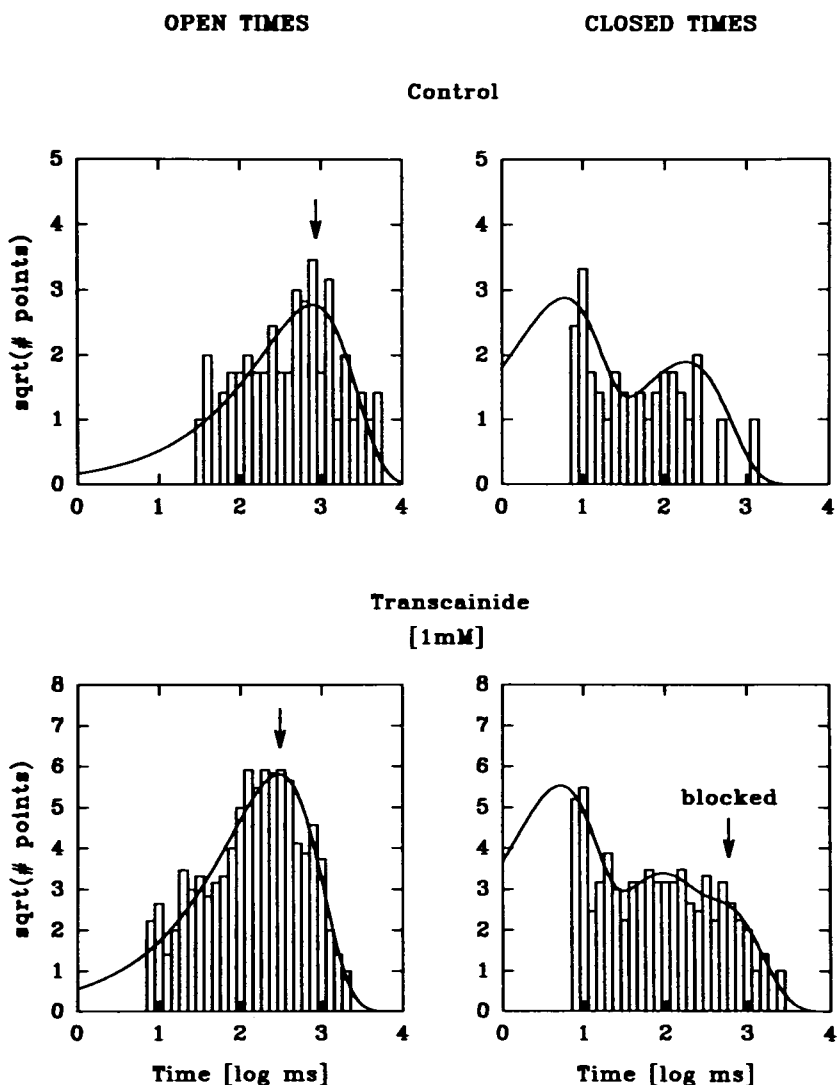


FIGURE 3 Dose dependence of the two blocking modes for BTX-activated bovine cardiac (●, —) and rat skeletal muscle (□, - - -) sodium channels at a membrane potential of  $-40$  mV. The data were fitted with the equations  $P_{\text{open}}(\text{apparent})/P_{\text{omax}} = 1 / \{1 + [T]/K_d(\text{slow})\}$  and  $I/I(\text{drug free}) = 1 / \{1 + [T]/K_d(\text{fast})\}$ , respectively, in panels A and B. The error bars in panel B indicate SDs. Note that the fit in A does not yield the true  $K_d$  for interaction between transcaïnide and the open channel during slow block (see Appendix). (A) Slow transcaïnide block: two typical examples of dose-response curves (from a total of eight) obtained from the normalized decrease in open probability. Slow block appears to follow 1:1 stoichiometry and is not tissue-specific. The  $K_d$  values obtained from the fits were 4.1 and 3.4 mM, respectively, for the cardiac and the skeletal muscle subtypes. Only data from one channel each are included in the figure. Both channels showed a similar control open probability,  $P_{\text{omax}}$ , of about 0.95, the plateau level approached by the activation curves in absence of the drug. (B) Fast transcaïnide block: dose-response curves were obtained by plotting the normalized single-channel conductance against transcaïnide concentration. Fast block follows 1:1 stoichiometry and does not appear to be tissue-specific. Data from three experiments for each channel subtype were included in the figure. The  $K_d$  values obtained from the fits were, respectively, 6.0 and 7.6 mM for the cardiac and the skeletal muscle channels.

FIGURE 4 Dwell-time distributions for a typical cardiac channel in absence and presence of 1 mM internal transcainide, plotted in the form devised by Sigworth and Sine (1987). In the absence of the drug, the open time distribution showed one resolvable component with a mean time of 786 ms. 1 mM internal transcainide decreased the apparent mean open time to 300 ms, suggesting that transcainide blocks the open channel. As expected for a BTX-activated cardiac channel, the closed time distribution showed two components under control conditions. Application of 1 mM transcainide resulted in the appearance of a distinct peak reflecting the blocked events. Time constants: [0 mM Transcainide]:  $t_{o1}$ (drug free) = 5.7 ms,  $t_{o2}$ (drug free) = 183 ms; [1 mM Transcainide]:  $t_{c1}$  = 5 ms,  $t_{c2}$  = 78 ms,  $t_b$  = 490 ms.



### Slow block is block of the open channel

Fig. 4 shows dwell-time histograms obtained from a BTX-activated bovine cardiac sodium channel in the absence and in the presence of 1 mM internal transcainide at a membrane potential of +40 mV. Under control conditions, the channel showed one resolvable open-time constant and at least two closed-time components. The slower closed-time component is characteristic of the BTX-activated cardiac subtype and is not seen for the skeletal muscle channels (French et al., 1990). Addition of 1 mM transcainide resulted in a decrease in mean open time, seen as a leftward shift of the open-time distribution. In four experiments at +40 mV, the open times were reduced to  $37 \pm 10\%$  (mean  $\pm$  SD) of their control values by 1 mM transcainide. In the closed-time distribution, an additional peak reflecting the blocked events became defined at about 400 ms. The inverse of this additional closed-time constant reflects the unblocking rate for slow transcainide block.

Fig. 5 shows the concentration dependence of the reciprocal mean open times and the reciprocal mean blocked times for a typical bovine cardiac sodium channel. The inverse of the mean open time increased linearly with transcainide concentration, whereas the mean blocked times were concentration-independent (probability of zero slope,  $P > 0.10$ ), suggesting that slow transcainide block is block of the open but not of the closed channel. The slope of the regression line for the mean open times reflects the apparent blocking rate constant for slow transcainide block, and the intercept reflects the rate of gating closure in the absence of the blocker.

Co-application of transcainide with other open-channel blockers, such as procainamide (1 experiment), QX-314 (2 experiments), or lidocaine (2 experiments), resulted in a reduced frequency of slow blocked events (data not shown). These observations support the idea that slow transcainide block occurs from the open channel, and that transcainide and the other compounds bind to a common site, which is not

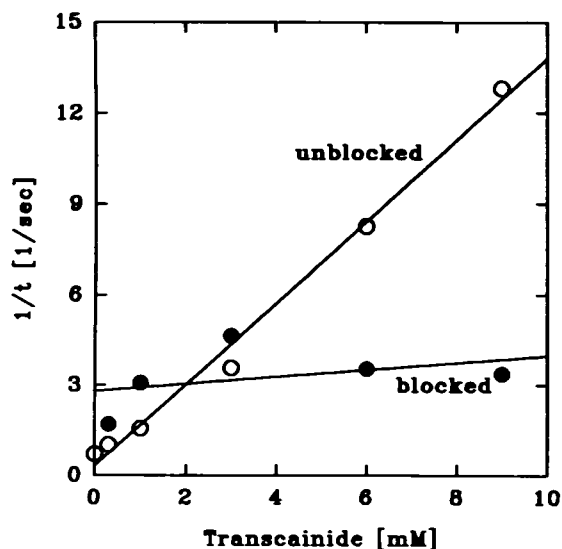


FIGURE 5 Dependence of the apparent mean open and the mean blocked times on the transcaïnide concentration. The data were taken from one bovine cardiac sodium channel. Solid lines are least-square fits. The inverse of the normalized mean open time ( $\circ$ ) increases with increasing drug concentration, whereas the mean closed time ( $\bullet$ ) appears to be little affected (slope = 0.11, probability of zero slope > 0.10). The data points were obtained from fits as in Fig. 4. The slope of the regression line for  $t_{\text{open}}$  reflects the apparent blocking rate for slow block of the apparent open state ( $1.3 \text{ mM}^{-1} \text{ s}^{-1}$ ), whereas the intercept at 0 mM transcaïnide reflects the sum of the gating transition rates from the open to the closed states in absence of the drug ( $0.3 \text{ s}^{-1}$ ).

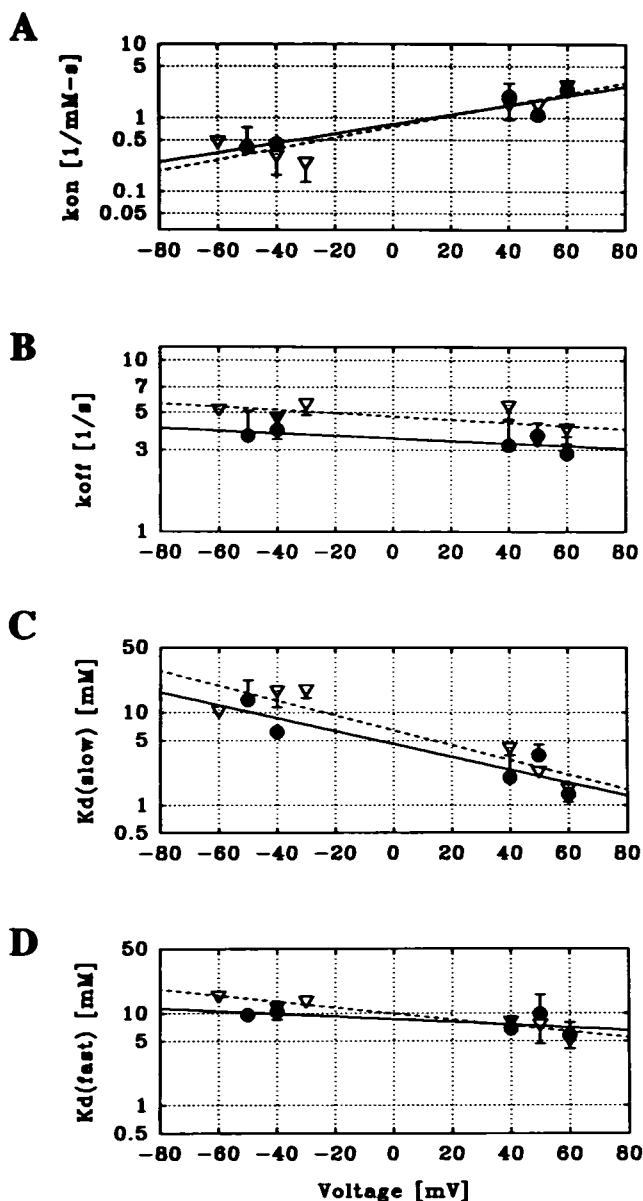
surprising given that transcaïnide is a lidocaine-derivative. Because fast block is also clearly open-channel block, we conclude that both blocking modes occur via drug binding to open channels.

### Fast and slow block differ in their sensitivities to voltage

Fig. 6 shows the voltage dependences of the individual apparent rate constants for slow block, as well as the voltage

FIGURE 6 Voltage dependences of the apparent rate and equilibrium dissociation constants for transcaïnide block of the cardiac ( $\bullet$ , —, upward error bars, 5 experiments for each type of block) and the muscle ( $\nabla$ , ---, downward error bars, 5 experiments for each type of block) subtypes. The regression lines are least-square fits; error bars indicate SDs. The rate constants were obtained from fits to dwell time histograms as in Fig. 4. (A) For slow block, the apparent blocking rates for both channel subtypes are favored by depolarizing potentials. (B) The unblocking rates for slow block are somewhat enhanced at hyperpolarizing potentials. (C) The apparent equilibrium dissociation constants for slow block (calculated from the ratio of the individual rate constants) for both channel types are increased with hyperpolarizing potentials. The slopes of the regression lines indicate that the charged amine group on the transcaïnide molecule enters the transmembrane voltage 40 and 47% of the way from the cytoplasmic side, respectively, for the cardiac and the skeletal muscle subtypes (Woodhull, 1973). (D) The equilibrium dissociation constant for fast block only weakly depends on the membrane potential. The slopes of the regression lines indicate that during fast block, the charged amine group enters the transmembrane voltage only 9 and 19% of the way from the intracellular side for the cardiac and the skeletal muscle subtypes, respectively.

dependences of the apparent equilibrium dissociation constants for slow and fast transcaïnide block. The apparent blocking rates for slow transcaïnide block (Fig. 6 A) were enhanced at depolarizing potentials, consistent with the idea of a positively charged blocker entering the transmembrane voltage from the cytoplasmic side of the channel. The apparent unblocking rates (Fig. 6 B) were slightly enhanced at hyperpolarizing voltages, as expected from a positively charged blocker exiting the transmembrane voltage toward the cytoplasmic side of the channel. The apparent equilibrium dissociation constant for slow block,  $K_d(\text{slow})$ , calculated from the ratio of the unblocking to the apparent blocking rate constants, was increased at negative membrane potentials. The steepness of the fits suggests that the charge on the transcaïnide molecule penetrates the transmembrane voltage 40 and 47% of the way from the cytoplasmic end of the channel (Woodhull, 1973) for the cardiac and the skeletal



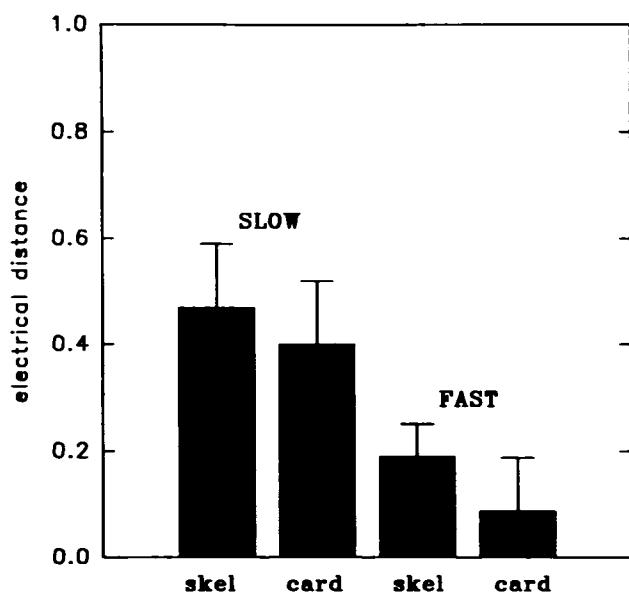


FIGURE 7 Comparison of the electrical distances for fast and slow transcainide block of the two channel subtypes. The filled bars indicate the electrical distances obtained from Fig. 6, C and D. The error bars indicate the 95% confidence intervals, calculated according to the formalism in Larsen and Marx (1981). The voltage dependences of fast and slow block differ significantly for each of the channel subtypes.

muscle channels, respectively. We note that the apparent blocking rate constants in Fig. 6 A (and the apparent  $K_d(\text{slow})$  values from Figs. 3 A and 6 C) describe the transitions from the apparent open state (which includes contributions from fast block) to the slow blocked state, rather than the rates of interaction with the true open state of the channel (see Appendix).

Fast block was too rapid to resolve the individual rate constants for block and unblock; however, the fractional decrease in apparent single-channel amplitude can be used to

calculate the equilibrium dissociation constant,  $K_d(\text{fast})$ , for fast block. Fig. 6 D shows the voltage dependence of the  $K_d(\text{fast})$  on the same ordinate as the  $K_d(\text{slow})$  in Fig. 6 C. The equilibrium dissociation constants for fast block were much less voltage-dependent than those of slow block. The steepness of the regression lines suggests that, during fast block, the positively charged amine group on the transcainide molecule penetrates the transmembrane voltage only 9 and 19% of the way from the cytoplasmic end of the channel for the cardiac and the skeletal muscle subtypes, respectively. Similar values (cardiac:  $z\delta = 0.06$ , skeletal muscle:  $z\delta = 0.15$ ) were obtained when we directly fitted the current reduction caused by 1 mM transcainide with a Boltzman function (not shown). In Fig. 7, we compare the electrical distances and their 95% confidence intervals for fast and slow transcainide block of the two channel subtypes. There is no overlap between the mean electrical distances and their 95% confidence intervals for either of the channel subtypes, indicating that the voltage dependences for fast and slow block differ significantly.

Fig. 8 illustrates the different voltage sensitivities of fast and slow block in form of single-channel records obtained from the same rat skeletal muscle channel at +40 and -40 mV. In absence of transcainide, the channel was open more than 95% of the time and showed a similar conductance at both voltages. Clearly, transcainide induced more blocked events at +40 mV, whereas the amplitude decrease differed less dramatically between the two potentials. This is graphically illustrated via the solid bars beside the records. For each record, the left bar indicates the normalized open probability, and the right bar indicates the fractional amplitude decrease on a scale from 0 to 1. Although slow block was more pronounced than fast block at +40 mV, the degree of fast block was greater at -40 mV, emphasizing that slow block was the more voltage-dependent process of the two.

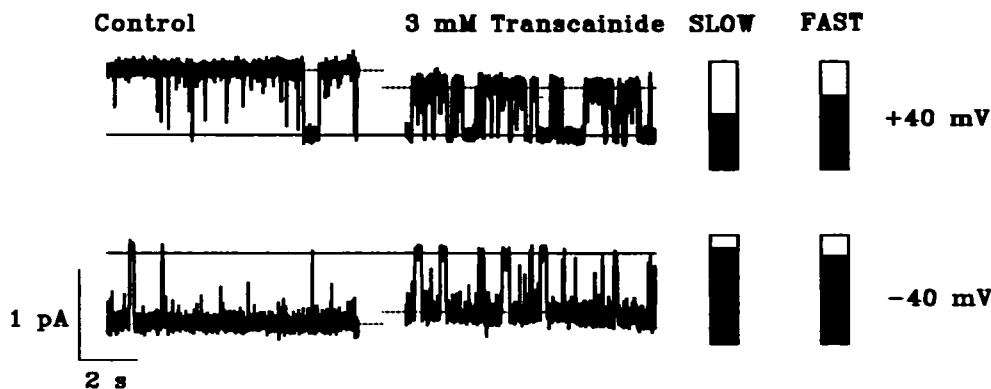


FIGURE 8 Single-channel records obtained from a BTX-activated skeletal muscle sodium channel in absence and presence of 3 mM transcainide at +40 and -40 mV. The solid lines indicate the closed level; the dashed lines indicate the apparent open levels. The solid bars reflect, on a scale from 0 to 1, the normalized open probability (SLOW:  $P_{\text{open}}(\text{apparent})/P_{\text{omax}}$ ) and the normalized single-channel conductance (FAST:  $g/g(\text{drug free})$ ) in the presence of transcainide. In the absence of transcainide, both channels showed a current amplitude of about 0.8 pA and were open about 95% of the time. Application of 3 mM transcainide resulted in pronounced slow block at +40 mV (the open probability dropped to about 50%), whereas at -40 mV slow block was much weaker (the open probability decreased to 0.88). In contrast, the single-channel amplitudes were reduced to 69 and 81% of the control amplitudes, respectively, at +40 and -40 mV, indicating that slow block was more voltage-dependent than fast block.

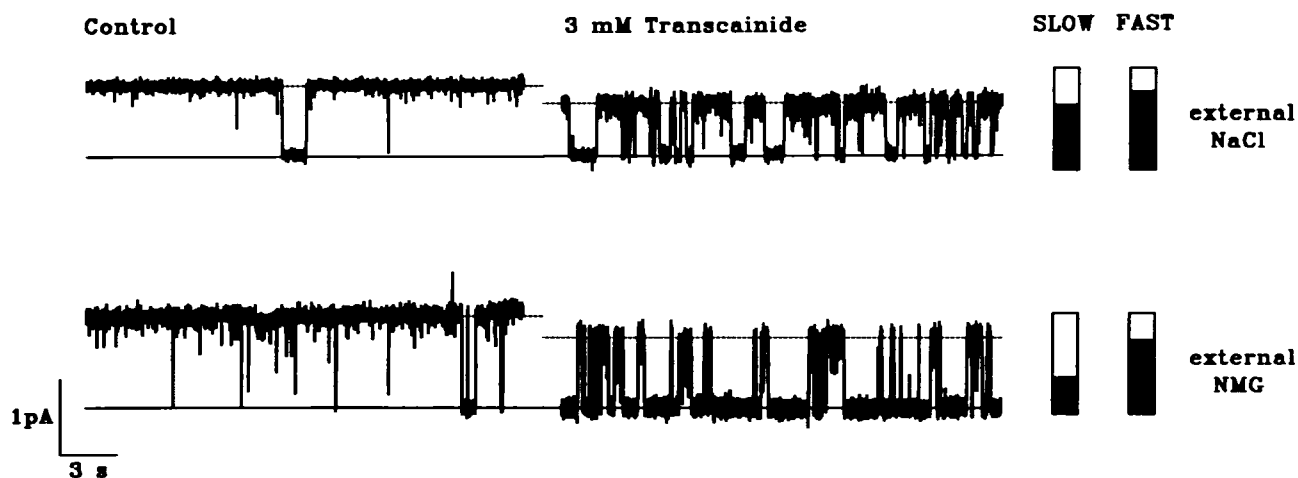


FIGURE 9 Single-channel records obtained from a BTX-activated bovine cardiac sodium channel in the presence and in the absence of 3 mM transcainide, in either symmetric 200 mM NaCl/20 mM MOPS (pH 7.0) or with 200 mM NMG/20 mM MOPS (pH 7.0) at the extracellular side. Lines and solid bars are as described in Fig. 8. The membrane potential was +40 mV. In the presence of external sodium ions, slow transcainide block reduces the apparent open probability and concomitantly reduces the apparent single-channel amplitude. Upon removal of external sodium ions, slow block becomes more pronounced, whereas fast block is only slightly affected (external NaCl:  $P_{\text{open}}(\text{apparent})/P_{\text{max}} = 0.65$ ,  $I/I(\text{drug free}) = 0.78$ ; external NMG:  $P_{\text{open}}(\text{apparent})/P_{\text{max}} = 0.38$ ,  $I/I(\text{drug free}) = 0.74$ ).

### Slow and fast block differ in their sensitivities to external sodium ions

Generally, open-channel block of sodium channels by amine local anesthetics is inhibited by external sodium ions (e.g., Zamponi et al., 1993a; Zamponi and French, 1993, 1994a (companion paper)). Because the transcainide molecule does not appear to enter deeply into the pore during fast block, one might expect fast block to be less sensitive to external sodium ions than slow block.

Fig. 9 examines the dependence of fast and slow transcainide block of a cardiac channel on external sodium ions at +40 mV. We recorded a control in symmetric 200 mM NaCl/20 mM MOPS (pH 7.0) and added 3 mM transcainide to the internal side. After determining the degree of block, the extracellular solution was replaced with 200 mM *N*-methyl-glucamine (NMG)/20 mM MOPS (pH 7.0). After block was observed under these conditions, transcainide was washed out to obtain a control record under the asymmetric ionic conditions. As can be seen from Fig. 9, the degree of slow transcainide block drastically increased upon removal of external sodium ions, with only little effect on fast transcainide block. In three experiments, the normalized open probability decreased from  $0.55 \pm 0.13$  to  $0.27 \pm 0.09$  when external sodium was removed, whereas the normalized single-channel amplitude decreased only from  $0.74 \pm 0.04$  to  $0.69 \pm 0.04$ . The latter values do not differ significantly at the 0.05 level. These data indicate that fast block does not sense external sodium ions, perhaps because transcainide does not deeply enter the pore during this type of block.

Overall, our data indicate that transcainide causes two modes of open-channel block that differ in their kinetics, their voltage dependences, and their sensitivities to external sodium ions.

### Additional observations: transcainide, batrachotoxin, and verapamil

In 10 out of 22 experiments, channels ceased to function within 5–30 min after transcainide application. This is atypical for batrachotoxin-activated sodium channels, which usually remain activated for several hours. A simple explanation is that transcainide speeds up batrachotoxin dissociation from the channel.

In five preliminary experiments on BTX-activated rat skeletal muscle sodium channels, verapamil, a calcium channel blocker and class IV antiarrhythmic agent (Camm et al., 1992), also caused two modes of open-channel block, one that was seen as discrete events, and a second type of block that appeared as a reduction in single-channel amplitude. Interestingly, unlike transcainide block, neither of the verapamil-blocking modes were strongly voltage-dependent. This compound thus deserves further attention. There may well be other structurally related blockers that have the ability to produce two types of open-channel block.

## DISCUSSION

### Two modes of open-channel block

Transcainide causes two distinct modes of open-channel block of BTX-activated sodium channels from both bovine heart and rat skeletal muscle: a rapid mode that is only weakly dependent on membrane potential, and a slower type of block that depends more strongly on voltage. The actions of transcainide differ from the fast and slow modes of lidocaine block (Zamponi et al., 1993a, b) in voltage sensitivity of the kinetic modes, in subtype specificity, and in state dependence. Slow lidocaine block is heart-specific, voltage-

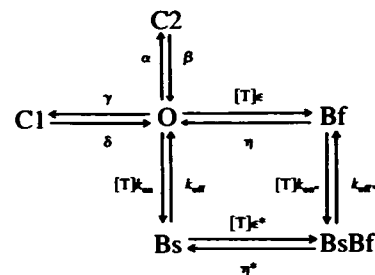
independent, and results from closed-state binding; fast lidocaine block is a subtype-independent, voltage-dependent, and results from open-state binding. Thus, transcainide shows a novel combination of blocking actions on BTX-activated sodium channels.

In the preceding paper (Zamponi and French, 1994a), we described the blocking actions of a series of lidocaine-related amines on BTX-activated cardiac channels. Two structurally very similar molecules, phenylmethylamine and phenylhydrazine, although both causing rapid open-channel block, differed drastically in the voltage dependences of their blocking actions. Phenylmethylamine blocked with a voltage dependence similar to that of slow transcainide block, whereas phenylhydrazine caused block that was similar, in its voltage dependence, to fast transcainide block. We argued that the charged terminal amine of phenylhydrazine, in contrast to other blockers, must be prevented from significant entry into the transmembrane electric field, probably because of this compound's relatively rigid structure.

During fast block by transcainide, the charged amino terminal of the transcainide molecule must be prevented from significant entry into the electric field, perhaps by the bulky structures in the aryl-amine link, leading to less stable and less voltage-dependent block, much like that of phenylhydrazine. In contrast, during slow block the charged amino terminal appears to penetrate more deeply, producing block with voltage-dependence similar to that of, for example, phenylmethylamine. Separate sites of action for the fast and slow block are further supported by the different sensitivities of

the two blocking modes to external sodium ions (Fig. 9) and by the kinetic analysis below.

Gingrich et al. (1993) recently reported two modes of open-channel block for the quaternary lidocaine derivative, QX-314. They suggested a scheme in which fast block was a requirement for slow block (see Scheme 4, Appendix). Gingrich et al. (1993) postulated that the QX-314 molecule enters the internal channel mouth in its fast-block conformation, and once the channel was fast-blocked, a re-orientation of the QX-314 molecule results in the more stable slow block, perhaps because of an additional hydrophobic interaction. The model proposed by Gingrich et al. (1993) did not fit our data (Fig. 10, and see Appendix). Indeed, none of the possible models based on a single molecule causing both fast and slow open-channel block (see Appendix) were able to account for our data. Only a kinetic model (Scheme 1) that allowed fast and slow block to occur noncompetitively appeared to fit satisfactorily our dose-response curves.



(Scheme 1, see also Appendix)

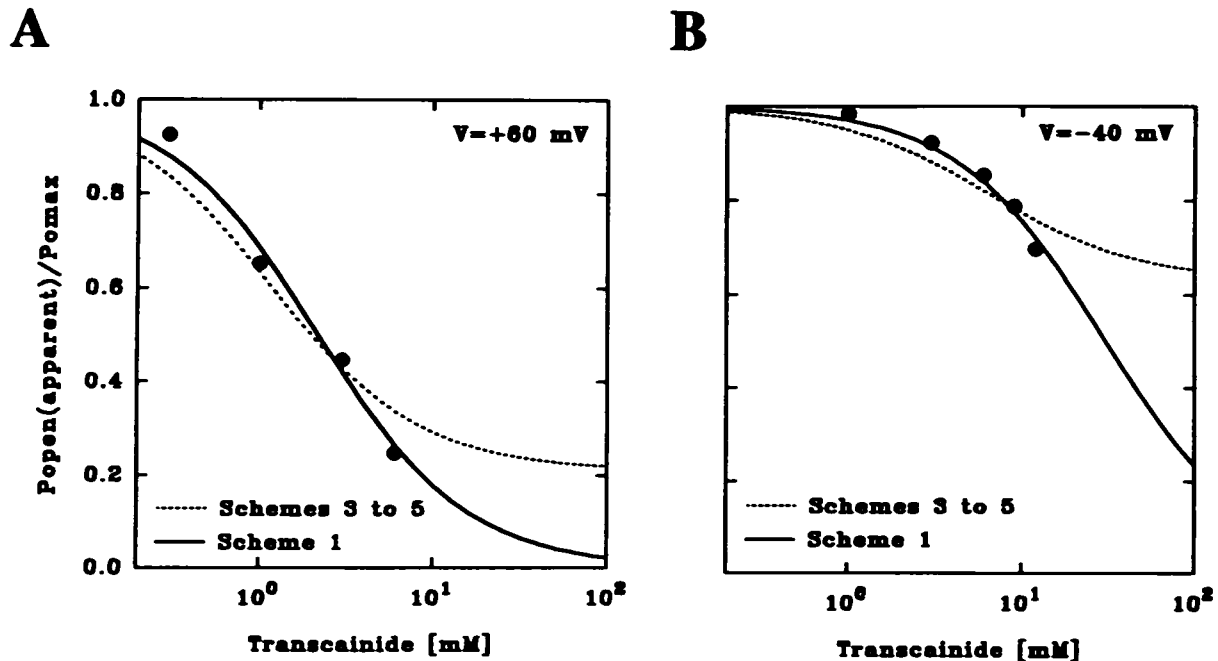


FIGURE 10 Fits of two examples of dose-response curves based on Schemes 3, 4, or 5 (---), as well as Scheme 1 (—), with the simplification that fast and slow block occur independently. The data were fitted according to the equations presented in the Appendix. The  $K_d(fast)$  values were obtained from each individual data set by fitting the transcainide-induced reduction in apparent single-channel conductance as in Fig. 3 B. Scheme 1, which allows fast-block and slow-block sites to be occupied simultaneously by separate transcainide molecules, yielded the best fits to both dose-response curves (fitting parameters: panel A,  $K_d(60$  mV) = 2.1 mM; panel B,  $K_d(-40$  mV) = 29.8 mM).



According to Scheme 1, block involves the actions of two transcaïnide molecules acting separately at the fast and the slow block sites. In this scheme, each site is accessible regardless of the occupancy of the other. Thus, slow block can occur from both the open and the fast-blocked states.

The detailed mechanism is not clear. When the channel is not fast-blocked, the transcaïnide molecule ( $pK_a = 8.9$ ) might be free to approach the slow blocking site via a hydrophilic pathway through the internal mouth of the channel in its charged form. For a fast-blocked channel, a direct hydrophilic access to the slow blocking site might be restricted, so that transcaïnide may have to approach the site via a hydrophobic route in its uncharged form (Hille, 1977; Zamponi et al., 1993a). A hydrophobic route would be consistent with the observation that transcaïnide acts similarly from either side of the membrane. An interfacial route, along which the protonated amino terminal remains exposed to the aqueous solution, whereas the more hydrophobic portion of molecule moves in a hydrophobic environment, is also conceivable. At this point, we cannot distinguish among the alternatives. Furthermore, it is possible that transcaïnide exists as two optical isomers with different blocking interactions. Regardless, our data suggest that the two blocking modes are effected at separate sites.

We have shown that phenylhydrazine block is sensitive to external sodium ions despite its weak voltage dependence (Zamponi and French, 1994a). In contrast, fast transcaïnide block was not significantly affected by external sodium ions. Together with the weak voltage dependence of fast transcaïnide block, this weakens the argument for a site within the conducting pathway. Thus, fast transcaïnide block and phenylhydrazine block could differ significantly at the molecular level.

Regardless of the detailed mechanism involved, we have identified two distinct modes of open-channel block by transcaïnide that appear to occur at two separate sites on the sodium channel. This action differs from QX-314 block which, to our knowledge, is the only molecule previously reported (Gingrich et al., 1993) to show two distinct modes of open-channel block of the sodium channel.

### Interactions with batrachotoxin

Transcaïnide application routinely resulted in the disappearance of channels from the bilayer, presumably because of batrachotoxin dissociation. It has been previously shown that local anesthetics and antiarrhythmics allosterically inhibit batrachotoxin binding (Postma and Catterall, 1984). However, lidocaine, which acts on BTX-activated sodium channels at concentrations similar to those required for transcaïnide block, does not cause loss of channels (Zamponi et al., 1993a), suggesting a more potent inhibition of BTX binding by transcaïnide. Because batrachotoxin is a relatively large molecule, one might expect that BTX interacts with the sodium channel at several micro-sites. A structural comparison between transcaïnide and batrachotoxin reveals that both

molecules (as well as other alkaloid channel activators such as veratridine) carry a saturated, hydroxylated ring (Coddington, 1983; Fig. 1). It is possible that the saturated rings of both molecules compete directly for one of these microsites, and if transcaïnide is successful, the overall stability of BTX binding is reduced, thereby increasing the rate of BTX dissociation. Such a mechanism would be supported by observations on the reversibility of transcaïnide block. In unmodified sodium channels, transcaïnide, but not lidocaine, causes irreversible block (Bennett et al., 1987), suggesting that, indeed, the rings attached to the aryl-amine link of transcaïnide interact strongly with unmodified channels. In our experiments, transcaïnide block was readily reversed upon wash-out, suggesting that batrachotoxin reciprocally weakens this interaction.

If portions of the BTX and transcaïnide molecules were indeed to compete for a site on the sodium channel, the BTX binding site would be located in the close vicinity of the class I antiarrhythmic binding site and, thus, the narrow region of the pore. This would enable a direct mechanism for previously reported effects of BTX on single-channel amplitude and ion selectivity (e.g., Quandt and Narahashi, 1982; Garber and Miller, 1987).

### Additional considerations

Transcaïnide has so far been little studied, and we know of no reports about transcaïnide action at the single-channel level. In one previous study, transcaïnide has been reported to be mainly an open-channel blocker (Carmeliet, 1988). This is consistent with our present findings. However, the study by Carmeliet was performed using macroscopic currents and, hence, it is not known whether transcaïnide also causes two modes of open-channel block in unmodified channels.

At +40 mV, transcaïnide is about 2 times more effective in blocking BTX-activated sodium channels than lidocaine (Zamponi et al., 1993a) and about 5 times more potent than QX-222 (Moczydlowski et al., 1986). Although having similar substituents on both its aromatic ring and its terminal nitrogen, the quaternary QX-222 lacks the ring structures attached to the aryl-amine link. Thus, these hydrophobic moieties attached to the aryl-amine link of transcaïnide appear to enhance transcaïnide binding, suggesting additional hydrophobic interactions besides those proposed in the preceding paper (Zamponi and French, 1994a).

The electrical distances obtained for fast, open-channel block by lidocaine, QX-314 (Zamponi and French, 1993), and QX-222 (Moczydlowski et al., 1986) were generally lower than those estimated for the simpler compounds used in the preceding paper (Zamponi et al., 1994a). This hints at the possibility that lidocaine and QX-314 cause two modes of open channel block, which are both rapid. If one of these modes were less voltage-dependent, the overall voltage dependence of fast lidocaine block would appear reduced. Our

experiments did not reveal two rapid open-channel blocking components for lidocaine (Zamponi et al., 1993a). Nevertheless, given the results by Gingrich et al. (1993) and our preliminary observations with verapamil, it is worth being aware that, at a wider bandwidth, other fast blockers might show a combination of blocking modes with different voltage sensitivities.

We thank Dr. John Daly for providing batrachotoxin, Drs. H. J. Duff and R. S. Sheldon for providing the transcainide, and Dr. Richard Horn for critical comments on the manuscript.

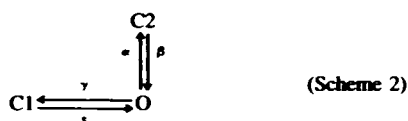
This work was supported by grants from the Medical Research Council of Canada and the National Institutes of Health, and from the Alberta Heritage Foundation for Medical Research in form of a Scholarship to R. J. French and a Studentship to G. W. Zamponi.

## APPENDIX

### Kinetic analysis

In this Appendix, we provide a mathematical description of the kinetic schemes used to fit dose-response curves. The mathematical treatment is formally carried out for block of the cardiac subtype. The formalism is analogous for the skeletal muscle channels, and the final expressions (Eqs. 6, 8, and 9) are identical for both channel subtypes.

In absence of blockers, BTX-activated cardiac sodium channels can be described via a linear three-state model:

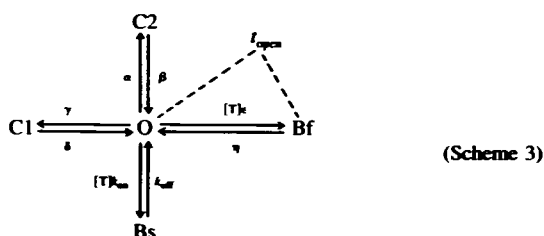


The closed state C1 is short-lived, voltage-dependent, and also seen with the skeletal muscle subtype; the closed state C2 is long-lived, voltage-independent, and a characteristic feature of BTX-activated cardiac sodium channels (French et al., 1990). In the absence of transcainide, at any given voltage, we define the control open probability of the channel,  $P_{\text{open}}$ , from Scheme 2, by the expression

$$P_{\text{open}} = \frac{1}{1 + \alpha/\beta + \gamma/\delta}. \quad (1)$$

Transcainide adds two additional kinetic states, a slow-blocked state, Bs, and a fast-blocked state, Bf. We considered four candidate kinetic schemes to describe the two observed modes of open-channel block by transcainide. Schemes 3–5 encompass all possible kinetic reactions for two modes of open-channel by a single transcainide molecule.

In the simplest model (Scheme 3), both fast and slow block occur from the open channel, without transitions between the two blocked states. According to Scheme 3, fast and slow block would antagonize each other. Moreover, either fast or slow block would prevent transitions to the two closed states C1 and C2. This appears to be a general property of open-channel amine blockers (Zamponi et al., 1993b; Zamponi and French, 1994b (companion paper)).



In Scheme 3, the probability of the open state,  $P_o(\text{true})$ , follows the expression

$$P_o(\text{true}) = \frac{1}{1 + \alpha/\beta + \gamma/\delta + \epsilon[T]/\eta + k_{\text{on}}[T]/k_{\text{off}}}, \quad (2)$$

where  $[T]$  is the transcainide concentration. The probability of being in the fast blocked state,  $P_f$ , is

$$P_f = P_{\text{open}}(\text{true}) \epsilon[T]/\eta. \quad (3)$$

The probability of being in the apparent open state,  $P_{\text{open}}(\text{apparent})$ , observed at a limited bandwidth that does not resolve discrete fast block transitions, is given by the sum of  $P_f$  and  $P_o(\text{true})$  and, hence,

$$P_{\text{open}}(\text{apparent}) = \frac{1 + \epsilon[T]/\eta}{1 + \alpha/\beta + \gamma/\delta + \epsilon[T]/\eta + k_{\text{on}}[T]/k_{\text{off}}}. \quad (4)$$

Combining Eqs. 1 and 4 yields

$$\frac{P_{\text{open}}(\text{apparent})}{P_{\text{open}}} = \frac{1 + \epsilon[T]/\eta}{1 + P_{\text{open}}(\epsilon[T]/\eta + k_{\text{on}}[T]/k_{\text{off}})}. \quad (5)$$

Equation 5 can be expressed using microscopic dissociation constants for the fast and slow block reactions,  $K_{\text{O-Bf}}$  and  $K_{\text{O-Bs}}$ :

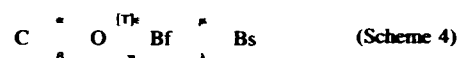
$$\frac{P_{\text{open}}(\text{apparent})}{P_{\text{open}}} = \frac{1 + [T]/K_{\text{O-Bf}}}{1 + P_{\text{open}}([T]/K_{\text{O-Bf}} + [T]/K_{\text{O-Bs}})}. \quad (6)$$

At very large transcainide concentrations, Eq. 6 becomes

$$P_{\text{open}}(\text{apparent}) = \frac{1}{1 + K_{\text{O-Bf}}/K_{\text{O-Bs}}}, \quad (7)$$

indicating that the channel reaches a constant open probability determined by the ratio of the equilibrium dissociation constants for fast and slow block. Equation 6 satisfactorily described only three out of eight dose-response curves; the remaining dose-response curves were ill fit, and data points consistently fell below the predicted plateau (see Fig. 10, *dashed lines*).

Two modes of cardiac sodium channel block by the quaternary lidocaine derivative, QX-314, have been reported by Gingrich et al. (1993) and described via the alternative linear model of Scheme 4. Here, a concentration-dependent fast block step is followed by a concentration-independent intramolecular reaction that results in binding to the slow block receptor.



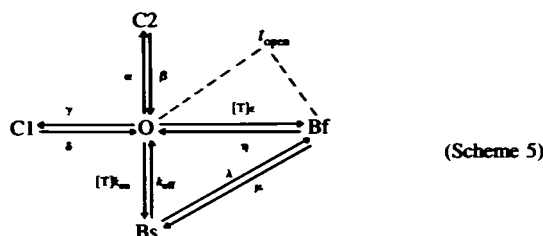
The derivation of the normalized open probability for Scheme 4 is analogous to the one presented above and yields

$$\frac{P_{\text{open}}(\text{apparent})}{P_{\text{open}}} = \frac{1 + [T]/K_{\text{O-Bf}}}{1 + P_{\text{open}}([T]/K_{\text{O-Bf}} + [T](K_{\text{O-Bf}}K_{\text{Bf-Bs}}))}. \quad (8)$$

However, a comparison with Eq. 6 indicates that both models yield identical expressions (the product  $K_{\text{O-Bf}}K_{\text{Bf-Bs}}$  in Eq. 8 can be replaced with a single constant, such as  $K_{\text{O-Bs}}$ ).

A combination of both models is obtained by permitting transitions between the two blocked states of Scheme 3. As in Scheme 4, the transition

from the fast-blocked state to the slow-blocked state is assumed to be concentration-independent.



(Scheme 5)

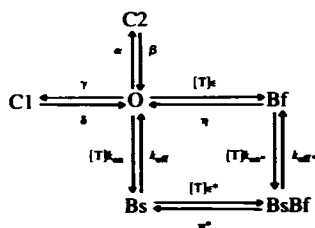
Assuming that  $\epsilon \gg k_{on}$ , and  $\eta \gg \mu$ , the normalized apparent open probability follows the expression

$$\frac{P_{open}(apparent)}{P_{max}} = \frac{1 + [T]/K_{O-Bf}}{1 + P_{max}([T]/K_{O-Bf} + B([T]/K_{O-Bf}))} \quad (9)$$

with  $A = \frac{1 + (\lambda/k_{off})(1/K_{Bf-Bs})}{1 + \lambda/k_{off}}$  and  $B = \frac{1}{1 + \lambda/k_{off}}$ .

Because both A and B are constant, this expression closely resembles Eqs. 6 and 8 and yields fits virtually identical to those from Schemes 3 and 4. Hence, we conclude that none of the models involving the action of single transcaïnide molecule can adequately describe our data.

The simplest model involving two individual transcaïnide molecules is shown in Scheme 1.



(Scheme 1, see Discussion)

Here, fast and slow block occur at separate sites, and the overall apparent voltage dependence observed for slow block would arise from a combination of the two slow blocking transitions. In the most general form, all of the rate constants are different. However, in our experiments, slow block appears as transitions from an apparent open state (a burst between O and Bf) to the slow-blocked state with apparent  $K_d(slow)$  values and apparent blocking rates that do not reflect the interactions between the transcaïnide molecule and the true open or fast-blocked states (Figs. 3 A and 6, A and C). Hence, we cannot resolve the individual microscopic transition rates between the various kinetic states, and the general form of Scheme 1 is of limited use for fitting our data. If fast and slow block are completely independent, we can set  $k_{on} = k_{on}$ ,  $k_{off} = k_{off}$ ,  $\epsilon = \epsilon^*$ , and  $\nu = \nu^*$ . This simplification yields a Michaelis-Menten dependence of the apparent normalized open probability on the transcaïnide concentration of the type

$$\frac{P_{open}(apparent)}{P_{max}} = \frac{1}{1 + [T]/K_d(slow)} \quad (10)$$

When we used the simplified model to fit the dose-response curves, the data were satisfactorily approximated (see Fig. 10). We note that the quality of the fits may likely be further improved if unequal transition rates are assumed. After all, given the close proximity of the fast and the slow blocking sites, it appears unlikely that a transcaïnide molecule approaching the fast

blocking site would not sense the presence of a second molecule at the slow blocking site, and vice versa. However, because our data do not permit us to resolve the relative contributions of both blocking pathways to the overall degree of slow block, we did not attempt to fit our data with the more general model.

Overall, we conclude that a single transcaïnide molecule cannot account for both modes of transcaïnide block, and although many other kinetic schemes are possible, a kinetic reaction such as in Scheme 1 appears to describe our data well.

## REFERENCES

- Bennett, P. B., R. Stroobandt, H. Kesteloot, and L. M. Hondeghem. 1987. Sodium channel block by a potent, new antiarrhythmic agent, transcaïnide, in guinea pig ventricular myocytes. *J. Cardiovasc. Pharmacol.* 9:661-667.
- Camm, A. J., H. A. Fozzard, M. J. Janse, R. Lazzara, M. R. Rosen, and P. J. Schwartz (for the Task Force of the Working Group on Arrhythmias of the European Society of Cardiology). 1991. The Sicilian gambit. A new approach to the classification of antiarrhythmic drugs based on their actions on arrhythmogenic mechanisms. *Circulation*. 84: 1831-1851.
- Carmeliet, E. 1988. Slowly developing activation block of cardiac sodium channels by a lidocaine analog, transcaïnide. *J. Cardiovasc. Pharmacol.* 12:110-115.
- CAST Investigators. 1989. Preliminary report: effect of encainide and flecainide on mortality in a randomized trial of arrhythmia suppression after myocardial infarction. *N. Engl. J. Med.* 321:406-412.
- Codding, P. W. 1983. Structural studies of sodium channel neurotoxins. 2. Crystal structure and absolute configuration of veratridine perchlorate. *J. Am. Chem. Soc.* 105:3172-3176.
- French, R. J., D. D. Doyle, L. Anscorn, M. C. Lee, K. J. Mather, and Y. Guo. 1990. Kinetic properties distinguish batrachotoxin-activated cardiac sodium channels from other subtypes in planar lipid bilayers. *Biophys. J.* 57:297a. (Abstr.)
- Garber, S. S., and C. Miller. 1987. Single  $Na^+$  channels activated by veratridine and batrachotoxin. *J. Gen. Physiol.* 89:459-480.
- Gingrich, K. J., D. Beardsley, and D. T. Yue. 1993. Ultra-deep blockade of  $Na^+$  channels by a quaternary ammonium ion: catalysis by a transition-intermediate state? *J. Physiol.* 471:319-341.
- Guo, X., A. Uehara, A. Ravindran, S. H. Bryant, S. Hall, and E. Moczydlowski. 1987. Kinetic basis for insensitivity to tetrodotoxin and saxitoxin in sodium channels of canine heart and denervated skeletal muscle. *Biochemistry*. 26:7546-7556.
- Hille, B. 1977. Local anesthetics: hydrophilic and hydrophobic pathways for the drug-receptor reaction. *J. Gen. Physiol.* 69:497-515.
- Krueger, B. K., J. F. Worley III, and R. J. French. 1983. Single sodium channels from rat brain incorporated into planar lipid membranes. *Nature*. 303:172-175.
- Larsen, R. L., and M. L. Marx. 1981. An Introduction to Mathematical Statistics and its Applications. Prentice-Hall, Englewood Cliffs, NJ. 596 pp.
- McManus, O. B., A. L. Blatz, and K. L. Magleby. 1987. Sampling, log binning, fitting, and plotting durations of open and shut intervals from single channels and the effects of noise. *Pflügers Arch.* 410:530-553.
- Moczydlowski, E., A. Uehara, X. Guo, and J. Heiny. 1986b. Isochannels and blocking modes of voltage-dependent sodium channels. *Ann. N.Y. Acad. Sci.* 479:269-292.
- Postma, S. W., and W. A. Catterall. 1984. Inhibition of binding of [ $^3H$ ]-batrachotoxinin A 20- $\alpha$ -benzoate to sodium channels by local anesthetics. *Mol. Pharmacol.* 25:219-227.
- Quandt, F. N., and T. Narahashi. 1982. Modification of  $Na^+$  channel currents by batrachotoxin. *Proc. Natl. Acad. Sci. USA*. 79:6732-6736.
- Sigworth, F. J., and S. M. Sine. 1987. Data transformations for improvement and fitting of single channel dwell time histograms. *Biophys. J.* 52: 1047-1054.
- Stroobandt, R., P. B. Bennett, L. M. Hondeghem, and H. Kesteloot. 1987. Evaluation of the efficacy and tolerance of the antiarrhythmic agent transcaïnide (R 54718). *Eur. J. Clin. Pharmacol.* 32:449-456.
- Wang, G. K. 1988. Cocaine-induced closures of single batrachotoxin-

- activated Na<sup>+</sup> channels in planar lipid bilayers. *J. Gen. Physiol.* 92: 747–765.
- Woodhull, A. 1973. Ionic blockage of sodium channels in nerve. *J. Gen. Physiol.* 61:687–708.
- Zamponi, G. W., D. D. Doyle, and R. J. French. 1993a. Fast lidocaine block of cardiac and skeletal muscle sodium channels. One site with two routes of access. *Biophys. J.* 65:80–90.
- Zamponi, G. W., and R. J. French. 1993. Dissecting lidocaine action: diethylamine and phenol mimic separate modes of lidocaine block of sodium channels from heart and skeletal muscle. *Biophys. J.* 65:2335–2347.
- Zamponi, G. W., and R. J. French. 1994a. Amine blockers of the cytoplasmic mouth of sodium channels. A small structural change can abolish voltage dependence. *Biophys. J.* 67:1015–1027.
- Zamponi, G. W., and R. J. French. 1994b. Open-channel block by tertiary amines inhibits activation gate closure in batrachotoxin-activated sodium channels. *Biophys. J.* 67:1040–1051.
- Zamponi, G. W., X. Sai, P. W. Coddling, and R. J. French. 1993b. Dual procainamide action on batrachotoxin-activated cardiac sodium channels. Open channel block and prevention of inactivation. *Biophys. J.* 65: 2324–2334.